Kinetic and Spectroscopic Investigations of Wild-Type and Mutant Forms of Apple 1-Aminocyclopropane-1-carboxylate Synthase†

Yishan Li, Liang Feng, and Jack F. Kirsch*

Department of Molecular and Cell Biology, Division of Biochemistry and Molecular Biology, University of California, Berkeley, California 94720

Received July 7, 1997; Revised Manuscript Received October 3, 1997⊗

ABSTRACT: Two catalytically inactive mutant forms of 1-aminocyclopropane-1-carboxylate (ACC) synthase, Y85A and K273A, were mixed in low concentrations of guanidine hydrochloride (GdnHCl). About 15% of the wild-type activity was recovered (theoretical 25% for a binomial distribution), proving that the functional unit of the enzyme is a dimer, or theoretically, a higher order oligomer. The enzyme catalyzes the conversion of *S*-adenosyl-L-methionine (SAM) to ACC. The value of k_{cat}/K_M is 1.2×10^6 M^{-1} s^{-1} at pH 8.3. Viscosity variation experiments with glycerol and sucrose as viscosogenic reagents showed that this reaction is nearly 100% diffusion controlled. The sensitivity to viscosity for the corresponding reaction of the less reactive Y233F mutant is much reduced, thus the latter reaction serves as a control for that of the wild-type enzyme. The k_{cat}/K_M *vs* pH profile for wild-type enzyme exhibits pK_a values of 7.5 and 8.9. The former is assigned to the pK_a of the α-amino group of SAM, while the latter corresponds to the independently determined spectrophotometric pK_a of the internal aldimine. The k_{cat} *vs* pH profile exhibits similar pK_as, which means that the above pK_a values are not perturbed in the Michaelis complex. The phenolic hydroxyl group of Tyr233 forms a hydrogen bond to the 3′-O^- of PLP. The spectral and kinetic pK_a (k_{cat}/K_M) values of the Y233F mutant are not identical (spectral 10.2, kinetic 8.7). A model that accounts quantitatively for these data posits two parallel pathways to the external aldimine for this mutant, the minor one has the α-amino group free base form of SAM reacting with the protonated imine form of the enzyme with $k_{cat}/K_M \approx 6.0 \times 10^3$ M^{-1} s^{-1}, while the major pathway involves reaction of the aldehyde form of PLP with SAM with $k_{cat}/K_M \approx 7.0 \times 10^5$ M^{-1} s^{-1}. The spectral pK_a is defined only by the less reactive species.

1-Aminocyclopropane-1-carboxylate synthase (*S*-adenosyl-L-methionine methylthioadenosine lyase, EC 4.4.1.14) catalyzes the synthesis of 1-aminocyclopropane-1-carboxylate (ACC)[1] from *S*-adenosyl-L-methionine (SAM) (Scheme 1). ACC is the immediate precursor to ethylene, the hormone that is responsible for fruit ripening and the regulation of many other developmental processes (*1*). The synthesis of ACC is the rate-determining step in the ethylene biosynthesis pathway (*1*). ACC synthase utilizes pyridoxal phosphate (PLP) as its coenzyme and is categorized as a member of the α subfamily of PLP-dependent enzymes that includes aspartate aminotransferase (AATase) (*2*). The proposed catalytic mechanism for this enzyme is an α,γ-elimination of enzyme-bound SAM (Scheme 2) (*3, 4*). The cDNA for ACC synthase has been cloned from various sources including tomato, winter squash, apple, and zucchini (*5*−*8*). The apple enzyme has been heterologously expressed in *Escherichia coli* and the active site characterized by site-directed mutagenesis (*9*). The recombinant enzyme has been crystallized and preliminary structural data reported (*10*).

The limited quantities of ACC synthase that can be isolated from natural sources (e.g., 1.4 mg of partially pure ACC synthase per 35 kg of apple fruits) (*11*) have severely hampered the progress of spectroscopic and mechanistic investigations of this enzyme. There is even controversy over the basic question as to whether this enzyme functions as monomer or dimer. Although most of the literature supports the dimer model (*8, 9, 12*), some evidence has been presented for an active monomer (*13, 14*).

Mechanistic analysis of many PLP-dependent enzymes are significantly facilitated by the spectral signatures of the different forms of the cofactor. For example, the pK_as in the k_{cat}/K_M *vs* pH profile for AATase have been assigned to the protonated internal aldimine, which has a $\lambda_{max} = 430$ nm, and the α-amino group of the substrate (*15*). The larger available quantities of ACC synthase allow similar investigations that lead to a striking but evolutionarily imperative result that enforces an elevated pK_a for the ACC synthase internal aldimine.

PLP-dependent mechanistic pathways include a number of chemically distinct intermediates. They are, in the present case, minimally the Michaelis complex, external aldimine with SAM, the stabilized C_α-carbanion (Scheme 2), the external aldimine with ACC, and the noncovalent product complex. A variety of mechanistic probes has been applied to define the free energy *vs* reaction coordinate landscape

† This work was supported by NIH Grant GM35393.

* Corresponding author.

⊗ Abstract published in *Advance ACS Abstracts,* November 15, 1997.

[1] Abbreviations: AATase, aspartate aminotransferase; ACC, 1-aminocyclopropane-1-carboxylate; AMPSO, 3-[(1,1-dimethyl-2-hydroxyethyl)amino]-2-hydroxy-1-propanesulfonic acid; CAPS, 3-(cyclohexylamino)-1-propanesulfonic acid; DTT, dithiothreitol; EDTA, ethylenediaminetetraacetic acid; GdnHCl, guanidine hydrochloride; MES, 4-morpholineethanesulfonic acid; MOPS, 4-morpholinepropanesulfonic acid; MTA, 5′-methylthioadenosine; MTI, 5′-methylthioinosine; PLP, pyridoxal 5′-phosphate; RdWT, sodium cyanoborohydride reduced wild-type; RT, room temperature; SAM, *S*-adenosyl-L-methionine; TAPS, 3-[[tris(hydroxymethyl)methyl]amino]-1-propanesulfonic acid; UV, ultraviolet; WT, wild-type.

S0006-2960(97)01625-5 CCC: $14.00

Scheme 1: Reaction Catalyzed by ACC Synthase

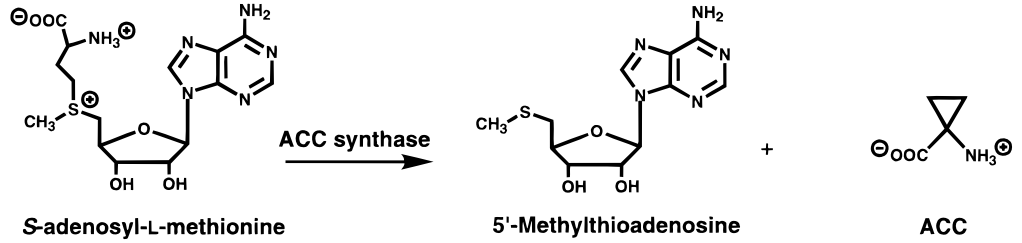

Scheme 2: α,γ-Elimination Mechanism of ACC Synthase

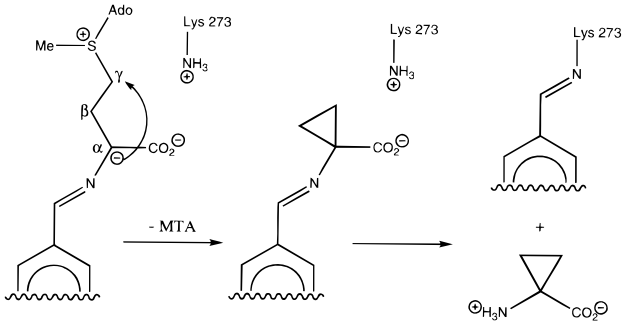

for AATase (*16*). Viscosity variation is particularly useful in delineating the contributions of diffusive steps (*17*−*19*). This technique is applied here to ACC synthase.

The 3′-O$^-$ of PLP is hydrogen bonded to the hydroxyl group of Tyr233 in ACC synthase. The Y233F mutant exhibits nearly the same value of k_{cat}, but a 24-fold increase in K_M compared to wild-type (*9*). The basis for these results is elucidated by comparative viscosity variation experiments and from an examination of the pH dependence of the spectral properties and steady state kinetic parameters of this mutant.

We report here conclusive proof obtained by inactive homodimer recombination experiments that ACC synthase does function only as a homodimer. The catalytic mechanism and spectral properties of the WT and active site Y233F mutant have been studied in order to elucidate the rate-determining steps in the reaction, the catalytically competent prototropic species, and the contribution of Tyr233 to catalysis.

MATERIALS AND METHODS

Materials. SAM was purchased from Calbiochem and used without further purification. 4-hydroxy-*N*-methylpiperidine was obtained from Lancaster and vacuum distilled before use. DEAE Sepharose Fast Flow and hydroxyapatite resin were from Pharmacia and Bio-Rad, respectively. Other chemicals and biochemicals were of the highest quality available commercially.

Methods. Bacteria strains BL21(DE3) pLysS containing expression vector pET with ACC synthase gene for WT, Y85A, Y233F, and K273A were available (*9*). The purification of WT ACC synthase and mutant enzymes was carried out according to the published procedure with yields ranging 1−3 mg of enzyme/Liter (*9*). Adenosine deaminase (Sigma catalog A 1907), the coupling enzyme, was purified as described previously (*9*).

Spectrophotometric Measurements and Steady State Kinetic Conditions. Spectrophotometric and kinetic measurements were conducted on Kontron Uvikon 860 or Perkin-Elmer Lambda 6 spectrophotometers. Steady state kinetics were monitored with the continuous assay system described previously (*9*). The concentration of SAM listed in the kinetic measurement conditions is the overall concentration prepared directly from the commercially available sample (from $\epsilon_{260nm} = 15\,400\ M^{-1}\ cm^{-1}$) unless otherwise specified. The material contains about 60% (*S*,*S*) SAM, whose concentration was determined enzymatically as previously described (*9*). The kinetic parameters k_{cat} and K_M were obtained from nonlinear regression fitting to the Michaelis−Menten equation with the KaleidaGraph program using the determined concentration of (*S*,*S*) SAM.

Reduction of WT ACC Synthase. The Schiff base of WT ACC synthase with PLP was reduced to a secondary amine with sodium cyanoborohydride ($NaBH_3CN$) (*20*, *21*). The reaction mixture contained 7.6 μM WT ACC synthase, 160 mM TAPS, pH 8.4, 10% glycerol, 10 μM PLP, and 25 mM $NaBH_3CN$. The progress of the reaction was monitored both spectrophotometrically at 425 nm and by activity assay.

Recombination of Enzyme Subunits. Subunit exchange between Y85A and K273A mutant enzymes in the absence of denaturants was carried out by mixing 170 μM Y85A with 170 μM K273A in buffer A (50 mM potassium phosphate, pH 8.4, 1 mM EDTA, 0.2 mM DTT, 10 μM PLP, and 15% glycerol) at room temperature (RT). The recovered activity was monitored by activity assay (100 μM SAM, 50 mM TAPS, pH 8.4, and 1 μM PLP at 25 °C). Hybridization experiments of Y85A with K273A and Y85A with reduced WT (RdWT) were carried out in buffer A at low concentration of GdnHCl to increase the rate of subunit exchange. The conditions were 170 μM Y85A, 170 μM K273A, and 0.125 M GdnHCl or 170 μM Y85A, 170 μM RdWT, and 0.25 M GdnHCl, both in buffer A for 24 h at RT. The mixture was subsequently dialyzed against buffer A with a microdialysis device at 4 °C for 24 h. The enzyme concentration was determined spectrophotometrically [$\epsilon_{280} = 1.55\ (mg/mL)^{-1}\ cm^{-1}$; (*9*)]. In order to evaluate the effect of the procedure on the enzyme, a control experiment with WT ACC synthase was always conducted along with the hybridization experiment under the same conditions.

Effects of Viscosity on the Kinetic Parameters for WT and Y233F. The relative viscosities ($\eta_{rel} = \eta/\eta^0$) of the buffer solutions containing 0−32% (w/w) sucrose or 0−32% (w/w) glycerol in 50 mM TAPS, pH 8.4, and 1 μM PLP were measured with an Ostwald viscometer at 25 °C (*17*). η^0 is defined as the viscosity of the buffer solution in the absence of added viscosogens.

Viscosity variation experiments were conducted in 7−500 μM SAM, 50 mM TAPS, pH 8.4, and 1 μM PLP at 25 °C for both WT and Y233F mutant enzymes. k_{cat} and K_M values were obtained from nonlinear regression fitting to the Michaelis−Menten equation.

Spectrophotometric pK_a Determinations. The pK_a of WT ACC synthase was determined using 14.4 μM enzyme in buffer containing initially 5 mM TAPS, pH 7.8, 0.5 M KCl, and 15% glycerol. The pH was varied by successive additions of 0.5 M AMPSO buffer (pH 10.6, $I_c = 0.5$) and 0.5 M CAPS buffer (pH 11.5, $I_c = 0.5$) above pH 9.3. The enzyme solution was drawn through a 0.2 μm filter to reduce light scattering from the small amount of precipitate. The absorbance and the pH of the solution were measured, and a correction was made to account for dilution. The data recorded at 435 nm and 373 nm were fitted to eq 1 and 2, respectively:

$$A = \frac{A_1 - A_2}{1 + 10^{(\mathrm{pH} - \mathrm{p}K_{\mathrm{spec}})}} + A_2 \quad (1)$$

$$A = \frac{A_1 - A_2}{1 + 10^{(\mathrm{p}K_{\mathrm{spec}} - \mathrm{pH})}} + A_2 \quad (2)$$

where A_1 and A_2 are the high or low absorbance limits at a particular wavelength, respectively. The spectra of Y233F at different pHs were recorded under the same conditions except that the enzyme concentration was 16.5 μM. The data recorded at 442 and 378 nm were fitted to eqs 1 and 2, respectively.

Evaluation of the pH Dependence of the Kinetic Parameters for WT and Y233F Mutant Enzymes. The buffer employed was the three component system that maintains constant ionic strength over the pH range of measurement (*22*). It contains 25 mM MES (pK_a 6.2), 25 mM MOPS (pK_a 7.2), and 50 mM 4-hydroxy-*N*-methylpiperidine (pK_a 9.7). The difference extinction coefficient ($\Delta\epsilon$) for methylthioadenosine (MTA) minus methylthioinosine (MTI) varies with pH and was determined spectrophotometrically in the same buffers.

The kinetic measurements for WT ACC synthase were carried out between pH 6.6 and 9.7 in the presence of 7−250 μM SAM and 1 μM PLP in the three component buffer system at 25 °C. k_{cat} and K_M values at each pH were obtained from nonlinear regression fitting to the Michaelis−Menten equation. Because the K_M for Y233F (290 μM) is 24-fold higher than that for WT (12 μM), the k_{cat}/K_M for Y233F at different pH values was obtained directly from the slope of a plot of velocity *vs* SAM concentration under [SAM] << K_M conditions. The SAM concentrations used for the kinetic measurements for Y233F were 9−30 μM in the same buffer as for WT.

The pH dependencies of k_{cat} and k_{cat}/K_M for WT enzyme were fitted to the bell-shaped curve described by eq 3:

$$Y = \frac{Y_{\mathrm{lim}}}{1 + 10^{(\mathrm{p}K_{a1} - \mathrm{pH})} + 10^{(\mathrm{pH} - \mathrm{p}K_{a2})}} \quad (3)$$

where Y_{lim} and Y are the upper limit and pH-dependent values, respectively, for the kinetic parameters. The pH dependencies of k_{cat} and k_{cat}/K_M for Y233F enzyme, however, were fitted to a 3 pK_a model (see Discussion).

Determination of the pK_a Value for the α-Amino Group of SAM. Successive aliquots of 30 mM KOH were added to 1 mL of 30 mM SAM in water. The pH was recorded after each addition, and a plot of the volume of KOH added *vs* pH was used to extract the pK_a for the α-amino group of SAM. A control experiment was carried out side by side with a methionine solution (30 mM). The (*S,S*) SAM contents of the sample before and after titration were determined enzymatically as previously described (*9*). The samples were also analyzed by electrospray mass spectroscopy before and after titration.

RESULTS

Reduction of WT ACC Synthase. The ϵ-amino group of Lys273 of WT ACC synthase forms a Schiff base with the carbonyl moiety of PLP (*20, 21*) resulting in the typical ~430 nm absorption peak observed at low pH for other PLP-dependent enzymes (*15, 23*−*25*). Reduction of these Schiff bases to the secondary amines eliminates that absorption peak. The absorbance of the protonated internal aldimine for WT ACC synthase with $\lambda_{max} = 420$ nm disappears upon treatment with 25 mM $NaBH_3CN$ for 24 h (data not shown). The completely reduced enzyme exhibits no measurable activity.

Formation of Heterodimers by Recombination of Subunits from Different Homodimers. There is disagreement in the literature concerning the existence of the active form of ACC synthase as a monomer (*13, 14*) or dimer (*8, 9, 12*) (see Discussion). Homology modeling and mutagenesis studies from this laboratory suggest that each active site of ACC synthase like those of aspartate aminotransferase has critical residues contributed by different subunits; therefore, the functional unit should be a dimer (*9*).

An *in vitro* proof for deciding the issue definitively originates from the work of Schachman's group (*26*). The strategy is diagrammed in Scheme 3. The K273A mutant enzyme has no detectable activity (*9*), and the Y85A form displays only 0.2% of the WT ACC synthase activity. Since active site residues Lys273 and Tyr85 are contributed from different subunits of the dimer in the model of White et al. (*9*), a single intact active site per dimer could be restored by hybridization of K273A and Y85A mutant enzymes. No activity would be recovered if Lys273 and Tyr85 were contributed by the same subunit to the active site nor if the active form was the monomer. Nonpreferential shuffling at a 1:1 ratio of K273A and Y85A should yield half of the dimeric population in heterodimeric form. Theoretically, the activity from a completely shuffled mixture of K273A and Y85A should be 25% of that of WT ACC synthase (1 active site/heterodimer X 50% of the population). Because the Schiff base formed by Lys273 and PLP was reduced in RdWT, it too displays no detectable activity. However, under the same scenario described for Y85A/K273A (Scheme 3), one intact active site per dimer should be formed in the Y85A/RdWT heterodimer.

Subunit recombination is normally expedited by low concentrations of protein denaturants (*27, 28*), but proceeds at a slow rate with ACC synthase even in their absence. About 5% of the WT activity was obtained after 72 h of coincubation of the Y85A and K273A homodimers (Figure 1).

The rate of recovery of activity is increased by low concentrations of GdnHCl. Recombination of Y85A with K273A and Y85A with RdWT was carried out in 0.125 M and 0.25 M GdnHCl in buffer A, respectively. WT activity at 15 and 7.1% (60% and 28.4% of the theoretical value, respectively) was recovered upon incubation of Y85A with K273A and Y85A with RdWT, respectively, after 24 h

Scheme 3: Recombination of the Inactive Monomers of ACC Synthase Y85A (Unshaded) and K273A (Shaded) To Form Dimers According to the Binomial Distribution[a]

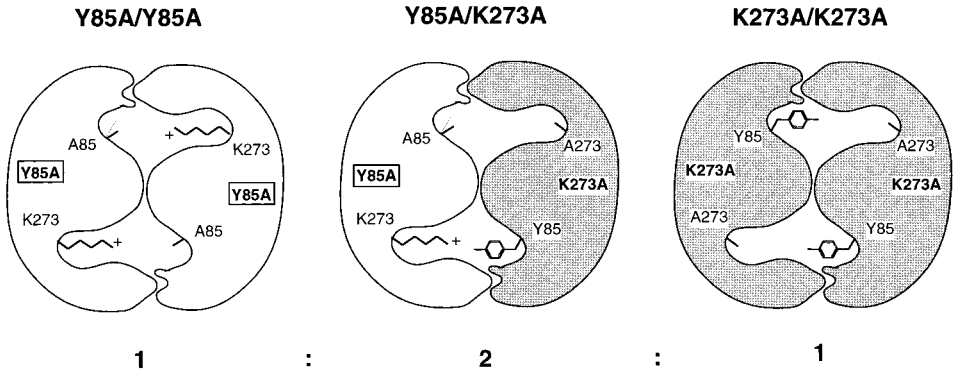

[a] Tyr85 and Lys273 are critical active site residues but are not contributed by the same monomer. The K273A homodimer has no detectable activity while the Y85A homodimer has only 0.2% of WT k_{cat}. The heterodimer contains one intact active site shown in the lower half of the center panel. Recombination therefore should result in the appearance of 25% of the WT activity if the active form of the enzyme is a dimer.

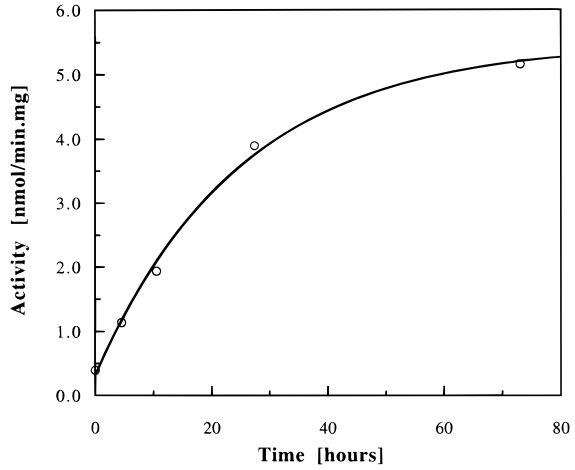

FIGURE 1: Recovery of activity from Y85A and K273A mutants of ACC synthase following the mixing of 11.0 μM Y85A and 11.0 μM K273A each in 50 mM K_2HPO_4, pH 8.4, 1 mM EDTA, 0.2 mM DTT, 10 μM PLP, and 15% glycerol. Specific activity was measured as described in Materials and Methods.

(Figure 2). These experiments establish unequivocally that the active form of the enzyme is a dimer. Some attempts were made to optimize the recovered yield further by varying the GdnHCl concentrations. Higher GdnHCl concentrations (>0.50 M) inactivate the WT control. The k_{cat} values for both hybrid enzymes are approximately equal to those calculated from the activity measurements, i.e., the two active sites within the dimer are independent. The K_M values for Y85A/K273A (19 μM) and Y85A/RdWT (20 μM) do not differ within error from that of the WT control (17 μM).

The Effect of Viscosity on k_{cat}/K_M. Quantitative analysis of the effects of viscosogens such as sucrose or glycerol on k_{cat}/K_M yields the extent to which an enzymatic reaction is diffusion controlled as well as the absolute value of the association rate constant. This procedure works best for enzymes that recognize a variety of substrates, only some of which are converted to products with near diffusion-controlled rate constants. The effects of viscosogens on the k_{cat}/K_M values for slowly transformed substrates serve as controls for their nonspecific effects on the enzyme alone (*17*). Knowles was the first to show that the procedure can also be applied to catalytically compromised mutant enzymes where the effects on the kinetics of the mutant enzyme serve as similar controls for a study of the rates of a possible diffusion-controlled reaction of WT enzyme with the natural substrate (*16*, *19*). The k_{cat}/K_M value for Y233F ACC synthase is 24-fold less than that of the WT enzyme. The high value of the latter rate constant (1.2×10^6 M^{-1} s^{-1}, see below) is consistent with that of a diffusion controlled reaction, while k_{cat}/K_M for Y233F is sufficiently reduced (5.1×10^4 M^{-1} s^{-1}) so that it is unlikely to represent a diffusion controlled reaction.

The normalized values showing the effects of viscosogens on k_{cat}/K_M are plotted according to eq 4b (*17*) where $(k_{cat}/K_M)^0$ and k_{cat}/K_M are the values of the parameter in the absence or presence of added viscosogens, respectively, and $P = k_{-1}^0/k_2$.

$$E + S \underset{k_{-1}}{\overset{k_1}{\rightleftharpoons}} ES \xrightarrow{k_2} E + P \tag{4a}$$

$$\frac{(k_{cat}/K_M)^0}{k_{cat}/K_M} = \frac{P}{1+P} + \frac{1}{1+P}\eta_{rel} \tag{4b}$$

The relative viscosities ($\eta_{rel} = \eta^o/\eta$) measured for 14, 24, and 32% (w/w) sucrose in 50 mM TAPS, pH 8.4, and 1 μM PLP at 25 °C are 1.5, 2.3, and 3.5, respectively. The η_{rel} values for 16, 24, and 32% (w/w) glycerol in the same conditions are 1.5, 1.9, and 2.5, respectively.

Neither viscosogen effects the difference extinction coefficient for MTA minus MTI significantly. The coupling enzyme concentrations employed were sufficiently high so that adenosine deaminase activity was not a rate-determining factor under the reaction conditions.

The effects of sucrose and glycerol mediated increases in viscosity on the values of k_{cat}/K_M for WT and Y233F mutant forms of ACC synthase are plotted in Figure 3. The slopes of the lines obtained in sucrose containing buffers are 1.20 and 0.22 for the WT and Y233F enzymes, respectively, while 1.51 and 0.50 are the corresponding figures found in glycerol solution. Preliminary experiments indicate that the values of k_{cat} for the Y233F mutant are much *more* sensitive to viscosity variation than are those for WT (data not shown), raising the possibility that product dissociation is partially rate determining for the reaction of the mutant enzyme.

Titration of the Internal Aldimine for WT and Y233F. The UV−visible spectra of the protonated internal aldimine of vitamin B_6-dependent enzymes exhibit absorption maxima

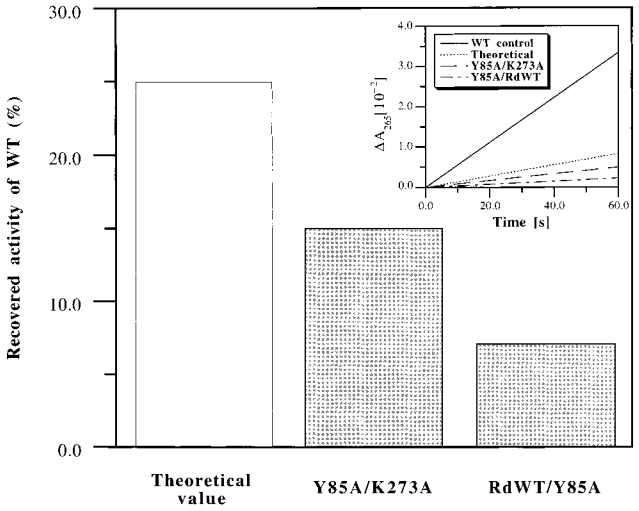

FIGURE 2: Percentages of the recovered activities from mixing Y85A with K273A (Y85A/K273A) and Y85A with RdWT (Y85A/RdWT) homodimers in comparison to that of WT control (shaded). Conditions for Y85A/K273A: 170 μM Y85A, 170 μM K273A, and 0.125 M GdnHCl in buffer described in Figure 1 at room temperature for 24 h. Conditions for Y85A/RdWT: 170 μM Y85A, 170 μM RdWT, and 0.25 M GdnHCl carried out as described for Y85A/K273A. The theoretical value (25%) from complete nonpreferential shuffling is indicated (unshaded). (Inset) The activities of WT control, Y85A/K273A, and Y85A/RdWT in terms of ΔA_{265} *vs* time (s). The theoretical activity from a complete nonpreferential shuffling is shown by the dotted line.

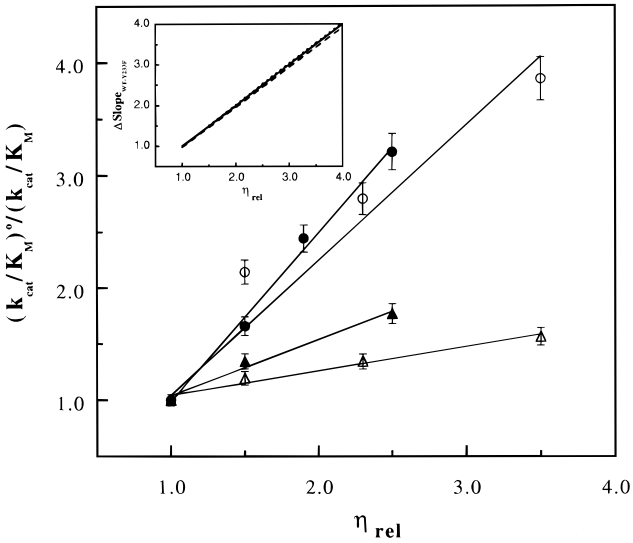

FIGURE 3: Plots of $(k_{cat}/K_M)^0/(k_{cat}/K_M)$ *vs* η_{rel} (eq 4b) for WT ACC synthase (circles) and Y233F mutant enzyme (triangles) in sucrose (open symbols) and glycerol (filled symbols) containing buffers (50 mM TAPS, pH 8.4, 1 μM PLP, and 25 °C). (Inset) Plots of $(k_{cat}/K_M)^0/(k_{cat}/K_M)$ *vs* η_{rel} with slopes of WT ACC synthase minus Y233F mutant enzyme in sucrose buffer (- - - -), of WT ACC synthase minus Y233F mutant enzyme in glycerol buffer (•••), and of the theoretical line of slope = 1.0 for a fully diffusion controlled reaction (—). The three lines are nearly superimposable.

near 430 nm while the deprotonated forms absorb typically near 360 nm (*23*, *24*) (Scheme 4). The low pH form of ACC synthase absorbs similarly at 420 nm; however, the maximum for the high pH form is found at 390 nm (Figure 4). The latter maximum is similar to that of the free aldehyde form of PLP and of the Y225F mutant form of AATase where the hydrogen bond bridging the phenolic OH and the 3′ hydroxyl group of PLP is eliminated (*25*). The UV spectrum of the internal aldimine has been particularly well characterized in AATase and follows the general pattern described above with the protonated form of the internal aldimine absorbing at 430 nm while the deprotonated form absorbs from 356 to 360 nm for WT enzyme (*15*, *25*, *29*, *30*). The spectrum of ACC synthase is also pH dependent. The λ_{max} value of the protonated form is 420 nm for WT ACC synthase, which is similar to that of AATase, while the unprotonated form of ACC synthase is red shifted by 30 nm to 390 nm in comparison to that of AATase (Scheme 4). The molar extinction coefficients for the 420 nm absorbing species at pH 7 and for the 373 nm absorbing species at pH 11 are the same for WT ACC synthase (6400 M^{-1} cm^{-1}, Figure 4). The molar extinction coefficient of the low pH form of the Y233F-ACC synthase mutant at 442 nm, however, is only 3600 M^{-1} cm^{-1} (Figure 5).

pH Dependence of the Kinetic Parameters. Specific salts and ionic strength have been shown to have major effects on the pH *vs* k_{cat} and k_{cat}/K_M profiles for AATase (*15*). These workers found that such perturbations were minimized in a three component buffer system (*22*); therefore, the pH dependence of the kinetic parameters of WT and Y233F ACC synthase was determined in similar buffers (25 mM MES, 25 mM MOPS, and 50 mM 4-hydroxy-*N*-methylpiperidine), which give a constant ionic strength (I_c = 0.050 M) from pH 6.5 to 10.0.

Reaction progress was monitored by the change in the differential absorbance between MTA and MTI (*9*). The MTI extinction coefficient is more pH sensitive than that of MTA. The difference extinction coefficients for MTA minus MTI at 265, 275, and 280 nm (280 nm not shown) were determined (Figure 6) and used in the data analysis. Curve fitting for $\epsilon_{MTA-MTI}$ to eq 1 yields pK_as of 9.0 ± 0.1 and 9.1 ± 0.1 at 265 and 275 nm, respectively. This pK_a arises from the deprotonation of the hydroxyl group at position-6 and its tautomer, the secondary amine group at position-1 of the inosine base rings.

Figure 7A shows the pH dependence of k_{cat}/K_M for the WT ACC synthase reaction. Nonlinear regression of the data on eq 3 yields acidic and alkaline pK_a values of 7.5 ± 0.1 and 8.9 ± 0.1, respectively (Table 1). This result indicates

Table 1: Spectrophotometric pK_a Values and pH dependence of the Kinetic Constants of WT and Y233F ACC Synthase[a]

		kinetic		limiting value		spectrophotometric
constant	enzyme	pK_{a1}	pK_{a2}	(M^{-1} s^{-1})	(s^{-1})	pK_{spec}[b]
k_{cat}/K_M	WT	7.5 (0.1)	8.9 (0.1)	1 200 000 (100 000)		9.26 (0.03)
k_{cat}/K_M	Y233F[c]	7.7 or 8.4	8.4 or 7.7	51 000 (4000)		10.2 (0.1)
k_{cat}	WT	7.4 (0.1)	9.3 (0.1)		11.0 (0.4)	

[a] The data fitted by these constants are shown in Figures 4, 5, 7, and 8. Standard errors are in parenthesis. Conditions are described in the figure legends and in the Materials and Methods. [b] The data shown are averages of the two values obtained at two wavelengths for WT (435 and 380 nm). The Y233F pK_a value was determined from titration at 442 nm only. [c] pK_{a1} = pK_{SAM}, and pK_{a2} = pK_{Lys} in eq 7. These two values are highly correlated, i.e., if pK_{SAM} = 7.7 then pK_{Lys} = 8.4 and *vice versa* (see Discussion).

Scheme 4: Postulated Role of the Ala224 (AATase) and Ile232 (ACC synthase) in Controlling the Free Energy of Hydrogen Bond Formation between Tyr225/233 and the 3′-O− of PLP[a]

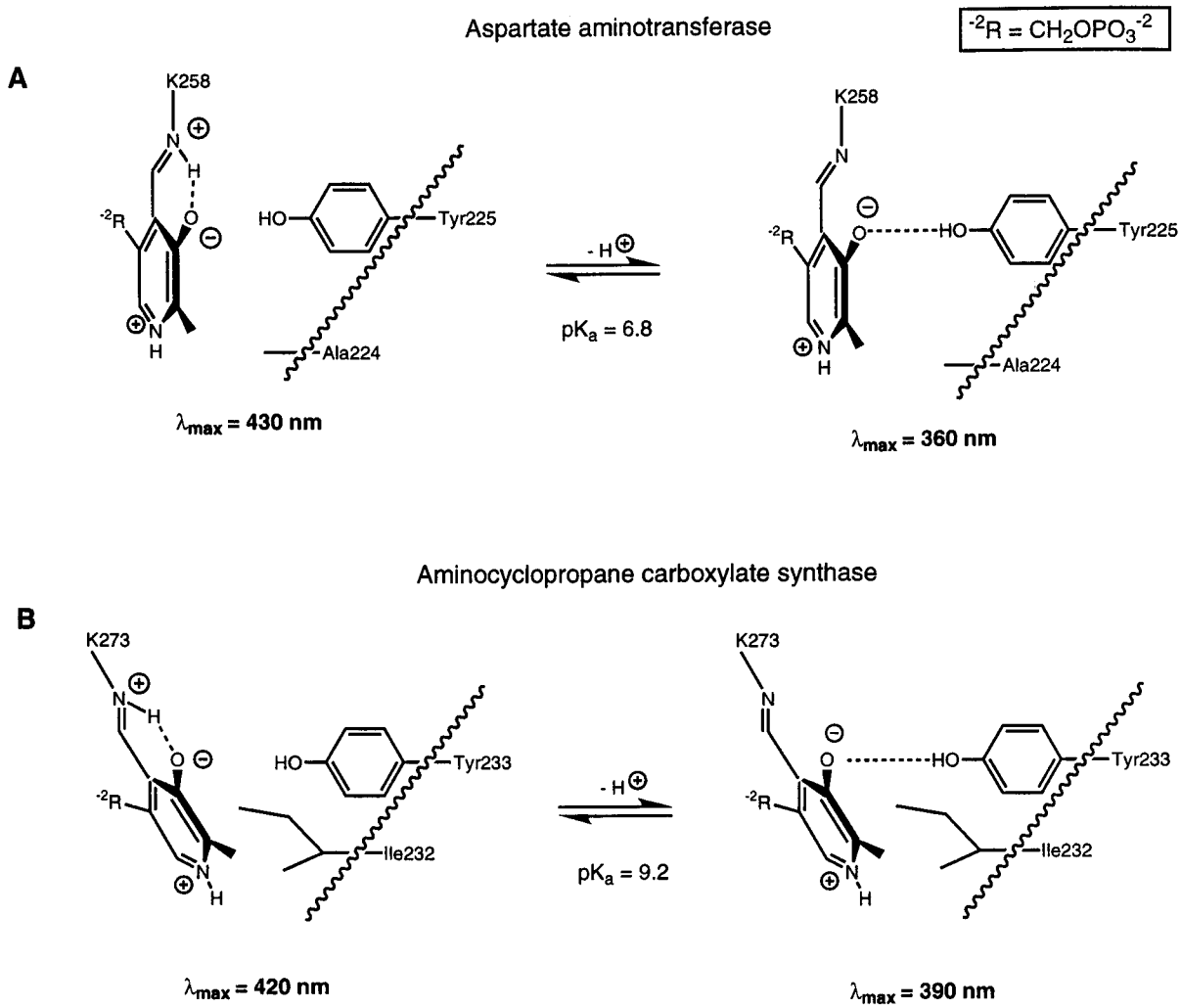

[a] The imine of AATase is more acidic because the small side chain of Ala224 permits a closer approach of the cofactor to Tyr225 with the formation of the strong hydrogen bond stabilizing the 3′-O⁻. The larger Ile-232 maintains a greater distance between the hydrogen-bonding parties; therefore, the anion is less stabilized and the pK_a is higher.

that the active species for free ACC synthase or free substrate includes a free base species with a conjugate acid pK_a of 7.5 and an acidic functionality with a pK_a of 8.9. The pH dependence of k_{cat} for WT ACC synthase is shown in Figure 7B. Curve fitting of the data reveals pK_a values of 7.4 ± 0.1 and 9.3 ± 0.1, similar to those controlling k_{cat}/K_M (Table 1). The data describing the pH dependence of k_{cat}/K_M for the Y233F-ACC synthase mutant are described by approximate pK_a values of 7.4 and 8.7 (Figure 8), but the curve of that figure was fit from a model different from that used for the WT enzyme kinetics (see Discussion).

The pK_a of the α*-Amino Group of SAM.* Gloss and Kirsch (*15*) have recently shown that the alkaline limb of the k_{cat}/K_M *vs* pH profile of AATase reflects the pK_a of the α-amino group of the substrate L-aspartate, which is 9.6. The pK_a of the α-amino group of SAM was determined by direct titration with KOH. The value is approximately 8.0, which is about 1.0 pH unit lower than that of methionine due to the electron-withdrawing nature of the sulfonium ion. It was recently reported that the pK_a of the α-amino group of *O*-acetylserine is 7.7 in comparison to 9.2 for that of serine (*31*), further illustrating the effect of an electron-withdrawing side chain on the pK_a of the α-amino groups of amino acid derivatives. SAM partly decomposes to MTA and α-amino-γ-butyrolactone (Scheme 5) during the titration, so the determined pK_a of 8.0 is imprecise. The lactone was identified by electrospray mass spectrometry (m/e = 102). The depurination decomposition pathway to give adenine and 5-*S*-ribosyl methionine (Scheme 5, m/e = 282) occurred to roughly the same extent as the lactonization reaction. The pK_a of the lactone should be close to that of glycine ethyl ester (7.75) (*32*), while that of the depurination product should be similar to that of SAM. Enzymatic assay before and after titration showed that 41% of the available (*S,S*) SAM decomposed during the titration from low to high pH (1.8−11.1).

DISCUSSION

ACC Synthase Functions as a Dimer. There is disagreement in the literature as to whether the functional unit of ACC synthase is a monomer or a dimer. Li and Mattoo (*13*) found that a 46−52 amino acid deletion in the C-terminal of the tomato ACC synthase, M_r = 52 kDa, runs as a monomer on gel filtration and exhibits higher specific activity than the WT enzyme, which is a dimer. They conclude that the monomeric form is "more active than the

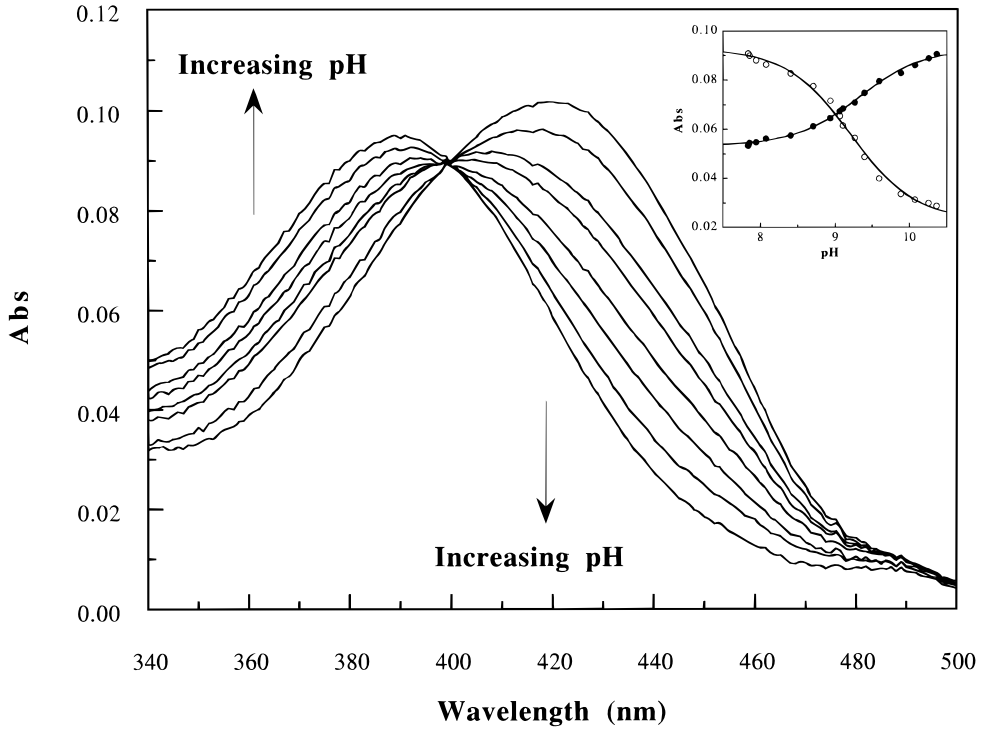

FIGURE 4: pH dependence of the UV−visible spectra of WT ACC synthase; pH 7.83, 8.40, 8.93, 9.06, 9.26, 9.39, 9.59, 9.88. (Inset) Theoretical fit of WT ACC synthase spectra according to eqs 1 and 2: 435 nm ($pK_{spec} = 9.21 \pm 0.03$, open circles, eq 1) and 373 nm ($pK_{spec} = 9.32 \pm 0.03$, filled circles, eq 2).

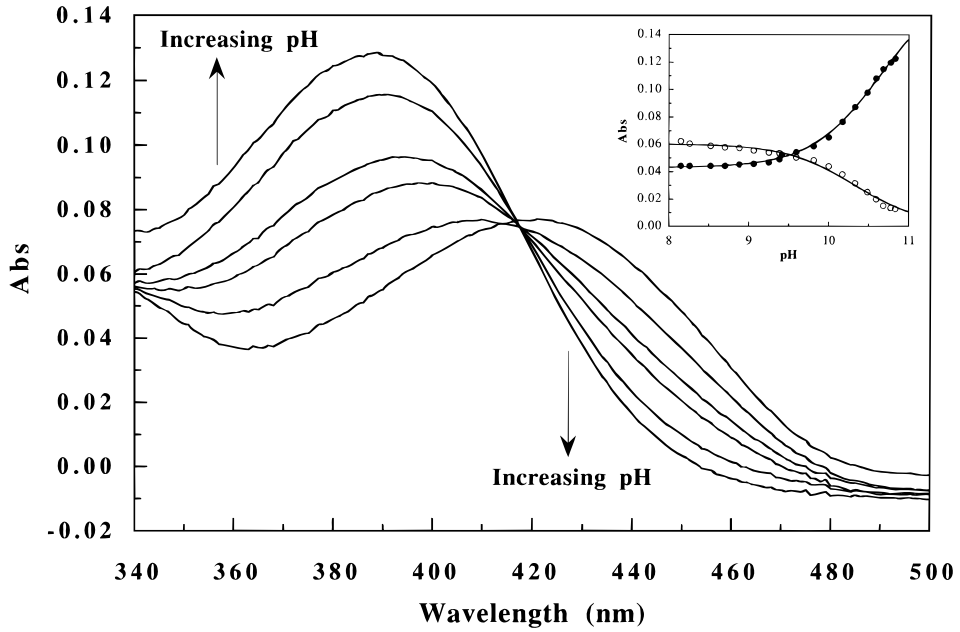

FIGURE 5: pH dependence of the UV−visible spectra of Y233F ACC synthase. pH 8.26, 9.81, 10.17, 10.33, 10.59, 10.83. (Inset) Theoretical fit of Y233F ACC synthase according to eq 1 and 2: 442 nm ($pK_{spec} = 10.2 \pm 0.1$, open circles, eq 1) and 378 nm ($pK_{spec} = 10.65 \pm 0.03$, filled circles, eq 2). The pK_a value of 10.2 is considered to be a better estimate because a lower boundary can be set ($A_2 \geq 0$). Therefore this value is used in the paper.

dimeric, full-length enzyme". Satoh et al. (*14*) also report ACC synthase activity associated with monomeric as well as dimeric forms of the tomato enzyme, whereas only dimeric and a higher oligomeric form of the enzyme from winter squash are active.

ACC synthase has about 10% sequence identity with AATase (*33*). Homology modeling identified the conserved active site residues shared by these two enzymes. The assignments were confirmed by site-directed mutagenesis (*9*). High-resolution X-ray structures of AATase are available [mitochondrial (*34*); cytosolic (*35*); *E. coli* (*36, 37*)]. All AATases are dimeric with two active sites per dimer. Both subunits contribute essential residues to each active site; therefore, AATase monomers are inactive. The site-directed mutagenesis experiments of White et al. (*9*) thus provide strong evidence that the functional unit of ACC synthase is also a dimer. These conclusions rest, however, on the assumption of the validity of the homology model.

The recovery of catalytic activity from hybridization of inactive or nearly inactive homodimers (Y85A/K273A and

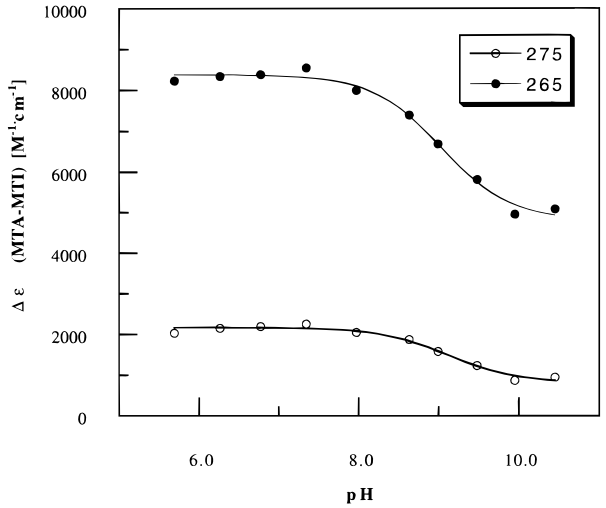

FIGURE 6: pH dependence of the difference extinction coefficient ($\Delta\epsilon_{5'-\text{methylthioadenosine}-5'-\text{methylthioinosine}}$) at 275 nm (open circles) and 265 nm (filled circles). The lines represent curve fitting of the data to eq 1. The three component buffer system is 25 mM MES, 25 mM MOPS, and 50 mM 4-hydroxyl-1-methyl-piperidine, $T = 25$ °C.

Y85A/RdWT) proves conclusively that the active form cannot be a monomer. The results also prove that the active site residues Lys273 and Tyr85 are contributed from different subunits as they are in AATase. Why are the catalytic activities of the hybrids less than the theoretical values of 25% of the WT? Three possible explanations can be considered. (1) The protein is irreversibly damaged by the GdnHCl treatment. This hypothesis is supported by the observation that only 60% of the WT enzyme activity is recovered in the control experiment. It is possible that one or both of the mutants and RdWT are even more susceptible to such damage. (2) Homologous association is thermodynamically favored over the heterologous one. This possibility is advanced because the changed amino acids are at the subunit surface. (3) Dissociation of the homologous subunit is incomplete under the experimental conditions. The enzyme tolerates only low concentrations of GdnHCl (e.g., the activity is reduced by 50% for WT enzyme in 0.25 M GdnHCl) without serious loss of activity. Explanation 3 is further supported by the observation that recovery is less when RdWT is substituted for K273A. The former is closely related to holoenzyme and cannot release coenzyme while the latter would likely dissociate PLP at very low [GdnHCl] leaving the labile apoenzyme, thus, accounting for the observed result. In fact, higher GdnHCl was required (0.25 M for the Y85A/RdWT hybridization experiment in comparison to 0.125 M needed to form Y85A/K273A) in order to maximize the yield of recovered active enzyme.

The nearly identical K_M values observed for Y85A/K273A and Y85A/RdWT to that of WT is another indication that the reconstructed active sites for both hybrid enzymes are the same as that of WT ACC synthase. Figure 1 shows that disproportionation occurs between dimers even in the absence of denaturant, demonstrating that the rate constant for dimer dissociation is relatively high ($t_{1/2} = 17.3$ h). Since the active site of ACC synthase embraces both subunits of the dimer, it is possible that the substrate induces dimerization by capturing the dimer selectively. This factor may help to explain the previous reports of active monomeric enzyme,

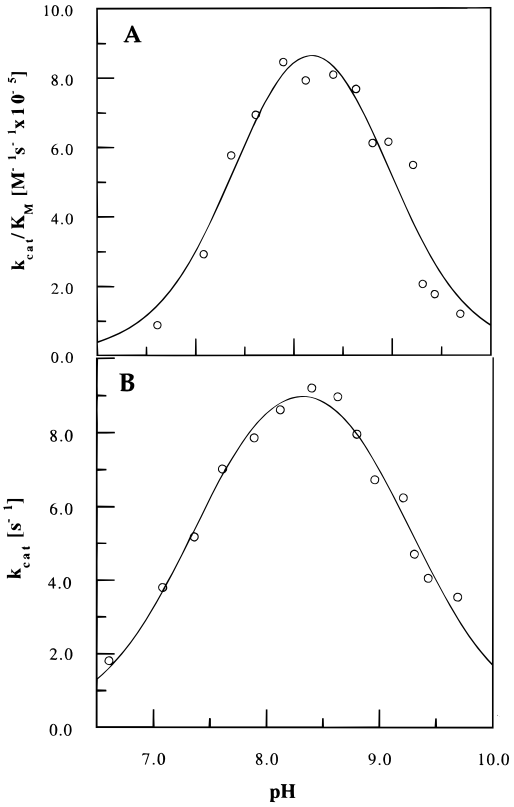

FIGURE 7: pH dependence of (A) k_{cat}/K_M for the WT ACC synthase catalyzed conversion of SAM to ACC. (B) k_{cat} for the WT reaction. The lines represent the nonlinear regression fit to eq 3. The fitted parameter values are given in Table 1. Conditions: 25 mM MES, 25 mM MOPS, 50 mM 4-hydroxy-1-methyl-piperidine, and 1 μM PLP, $T = 25$ °C. SAM was 7−250 μM (A and B).

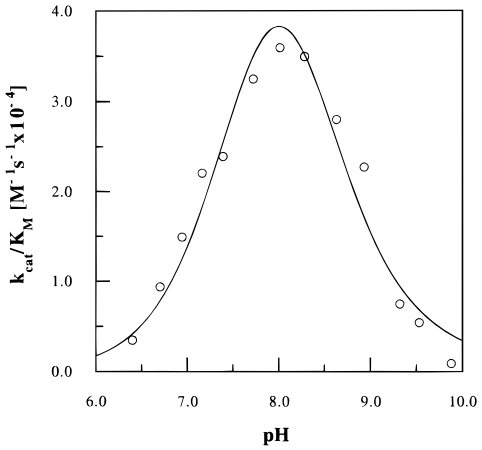

FIGURE 8: pH dependence of k_{cat}/K_M for Y233F ACC synthase. The line represents the non-linear regression fit to a three pK_a model described by eq 7, where K_{eq}, pK_{SAM}, and pK_{spec} are set to 1.0, 8.3, and 10.2, respectively. The range of fitted parameters from simulations is given in Table 3. Experimental conditions are the same as those of WT except that the SAM concentration was 15−20 μM. The value of k_{cat}/K_M for Y233F mutant enzyme at each pH was obtained from the slope of $v = (k_{cat}/K_M)[S]$ with $[S] << K_M$.

i.e., the monomer/dimer equilibria were measured in the absence of substrate (see above) (*13*, *14*).

The WT ACC Synthase Reaction is Diffusion Controlled. The slope of a $(k_{cat}/K_M)_{rel}$ $[=(k_{cat}/K_M)^0/(k_{cat}/K_M)]$ *vs* η_{rel} plot should be 1.00 for a fully diffusion controlled reaction. Partially diffusion controlled reactions are characterized by $0 <$ slope < 1.00 (see, e.g., ref 17). The slopes of plots of $(k_{cat}/K_M)_{rel}$ *vs* η_{rel} for the reactions of WT ACC synthase with

Scheme 5: Proposed Routes for the Principle Modes of Nonenzymatic Decomposition of the Neutral Form of SAM[a]

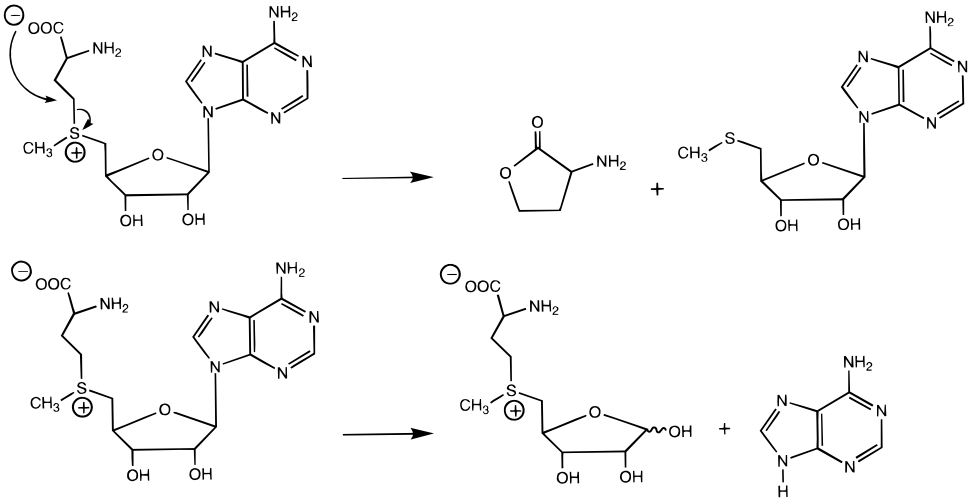

[a] The product ratios indicate roughly equal fluxes through each pathway.

SAM in sucrose and glycerol containing buffers of 1.20 and 1.51, respectively, are higher than the theoretical limits. These figures demonstrate the necessity for control reactions specific to the interpretation of viscosity variation experiments (*18*). The high concentration of viscosogenic reagents employed may cause changes in the enzyme structure that become manifest in kinetic or equilibrium constants aside from those rate constants for substrate association/dissociation. This limitation has been addressed in two ways-evaluation of the nondiffusive perturbation by measuring (1) the effects of at least two viscosogens on WT enzymes that recognize a variety of substrates, some of which are transformed to products with chemically controlled rate constants; these data provide direct measures of the nonspecific effects induced by the viscosogens (*17*, *18*, *38*, *39*); and (2) the effects of mutations that substantially decrease the activity of WT enzyme to the extent that reactions that proceed with candidate diffusion controlled rate constants for the WT enzyme are slowed to where the same reactions are governed by chemically controlled rate constants in the mutant enzymes (*16*, *19*). The high values of the slopes of the plots of k_{cat}/K_M *vs* η_{rel} for WT ACC synthase support the hypothesis that the rate constant for association with SAM is diffusion controlled; however, that for the corresponding reaction with the Y233F mutant is 24-fold less and is, thus, likely to reflect chemical rather than diffusion steps. The analogous mutation in AATase (Y225F) has been shown to convert that enzyme from one whose rate of reaction with oxalacetate is partly diffusion controlled in WT to one where the rate is completely chemically limiting (*16*). The slopes of the normalized values of plots of k_{cat}/K_M *vs* η_{rel} for Y233F ACC synthase are 0.22 and 0.50 for sucrose and glycerol, respectively. These nonzero figures quantitate the nonspecific effects of the viscosogens on ACC synthase. Their subtraction from the WT slopes in Figure 3 isolates the effects of the viscosogens to the diffusive steps. The resulting values of the slopes are both very nearly equal to unity, indicating that the sole rate-determining step in k_{cat}/K_M is the association of SAM with the WT enzyme. The nonspecific effects generated by the sucrose control (slope = 0.22) are less than those effected by glycerol (0.50), yet subtraction of these values from those recorded for the WT enzyme yields the identical result of unit slope, further confirming the validity of this approach to the determination of diffusion controlled rate constants. The association rate constant in this instance is therefore equal to the value of $k_{cat}/K_M = 1.2 \times 10^6\ M^{-1}\ s^{-1}$ at the optimum pH of 8.3. The effects of viscosogens on k_{cat} for WT and Y233F mutant forms are different from those observed for k_{cat}/K_M. Preliminary data (not shown) show that the values of k_{cat}, by contrast, are insensitive to glycerol or sucrose concentration, while those for the Y233F mutant enzyme are more so. These observations suggest that release of product may be a component of k_{cat} for the Y233F mutant enzyme.

Why is the wild-type reaction diffusion controlled while that of Y233F is not? The first steps of the reaction are shown in eq 5:

$$\text{SAM} + \text{ACC synthase} \underset{k_{-1}}{\overset{k_1}{\rightleftharpoons}} \text{External Aldimine} \xrightarrow{k_2} \text{Product} \quad (5)$$

where k_1 represents the rate constant for association of SAM with the enzyme, k_{-1} the dissociation rate constant, and k_2 the combined rate constant for all kinetically consequential steps following association (k_{cat}); k_{cat} is nearly the same for wild-type and mutant enzyme; therefore, the mutation does not effect these steps. The value of K_M for this simple model is given by

$$K_M = \frac{k_{-1} + k_2}{k_1} \quad (6)$$

The inequality $k_2 >> k_{-1}$ holds for WT, but $k_{-1} >> k_2$ for Y233F mutant enzyme. It is less likely that the mutation will perturb k_1, which represents diffusion of the substrate to the enzyme, so the probable consequence of the mutation is to decrease the stability of the Michaelis complex, and/or external aldimine, by increasing k_{-1} by 625-fold. The value of k_{-1} for the WT enzyme must be <20% of k_{cat} or $<2\ s^{-1}$. The small value is a consequence of the many favorable interactions of SAM with the active site.

Identification of the Reactive Protonic Forms of ACC Synthase and SAM. The k_{cat}/K_M *vs* pH profile of WT AATase exhibits ascending and descending limbs of 6.9 and 9.6, respectively, which have been assigned to the internal

Scheme 6: Comparison of the pK_a Values of the Amino Acids and Internal Aldimines for AATase and ACC Synthase[a]

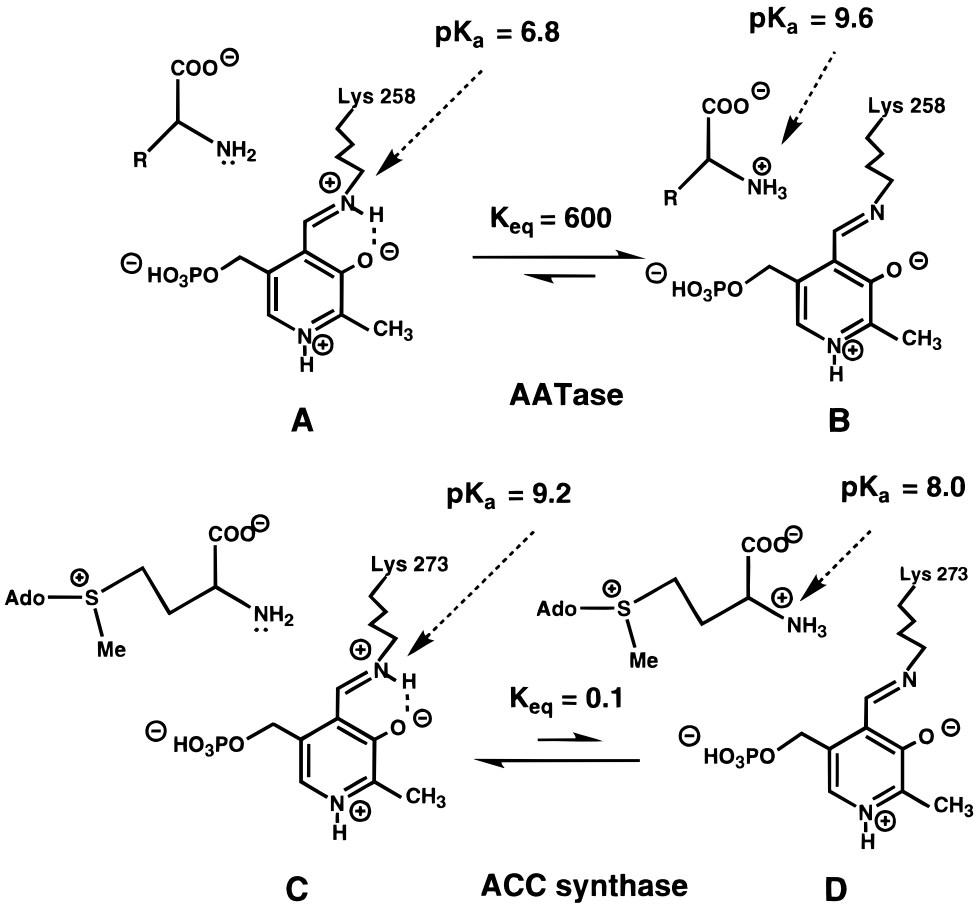

[a] The thermodynamically most populated forms of the AATase reactants near neutral pH are shown in panel B, but those for the ACC synthase reactants are represented in panel C.

aldimine and the amino acid, respectively (*15*). The most populated forms of the *free* enzyme and *free* amino acid in the pH 7−9 range are shown as structure B in Scheme 6. The chemistry of the transaldimination reaction, however, requires that the free base form of the α-amino group attack the protonated imine (Scheme 6, structure A) (*40*). The ratio of [A]/[B], as calculated from the pK_as is 1/600; therefore, the minimum value for the rate constant for association of L-Asp with AATase is $600 \times (k_{cat}/K_M^{Asp}) = 4.1 \times 10^7$ M^{-1} s^{-1} if the reaction occurs through the protonic configuration of the reactants shown in Scheme 6A. The question of whether the Michaelis complex is formed by reaction of the protonic configuration of Scheme 6A *vs* that of 6B cannot be resolved by kinetics, which can only define the number of protons involved in a reaction, not their location. Whatever the mechanism, the reaction is not diffusion controlled, as there is no appreciable effect of relative viscosity on k_{cat}/K_M^{Asp} (*16*).

The important pK_a values in the ACC synthase reaction are reversed, i.e., that of the internal aldimine is 9.26 ± 0.03 and that of SAM is 8.0 ± 0.2, both of which were determined by direct titration. The kinetic pK_as reflected in the WT ACC synthase k_{cat}/K_M *vs* pH profile of (7.5 and 8.9) are in reasonable agreement with those determined by titration. Thus, the reacting protonic configuration of WT ACC synthase combining with SAM is the thermodynamically more populated one (Scheme 6, structure C) in contrast to the AATase reaction. The ACC synthase reaction is diffusion controlled (see Results), because of the excess "stickiness" of SAM for ACC synthase compared to that of L-Asp for AATase. From an evolutionary standpoint it is selectively advantageous for the pK_a of the internal aldimine to be raised to ≈9 to offset the low pK_a of SAM in order to increase the population of the reactive species near physiological pH. For example the value of k_{cat}/K_M at pH 8 would be reduced about 10-fold were the pK_a of the aldimine equal to 7 as it is in AATase.

The Effect of the Y233F Mutation in ACC synthase. The phenomenological consequences of the Y233F mutation in ACC synthase are qualitatively different from those of the corresponding Y225F mutation in AATase. First, the k_{cat} of Y225F-AATase is decreased by 400-fold compared to that of the WT, while the k_{cat} of Y233F-ACC synthase is about the same as that of the WT enzyme. The K_M of the Y225F-AATase/L-Asp complex is also decreased by 20-fold, while the K_M of the Y233F-ACC synthase/SAM complex is *increased* about 24-fold. The explanation for the AATase result was presented in terms of a tug-of-war model (Scheme 4A) where the H-bond to Tyr225 pulls the PLP against Ala224 at the back of the PLP binding pocket. Combination of the enzyme with the substrate amino acid weakens the H-bond substantially at a cost of some free energy; therefore, K_M is lower in the mutant where the hydrogen bond is lacking. The catalytically active conformation of the external aldimine requires re-establishment of that H-bond; therefore, the mutant has a lower k_{cat} (*25*).

The position of Ala224 in AATase is taken by the larger Ile232 in ACC synthase; thus, the H-bond between Tyr233

Scheme 7: Equilibria Associated with WT and Y233F Holo ACC Synthases[a]

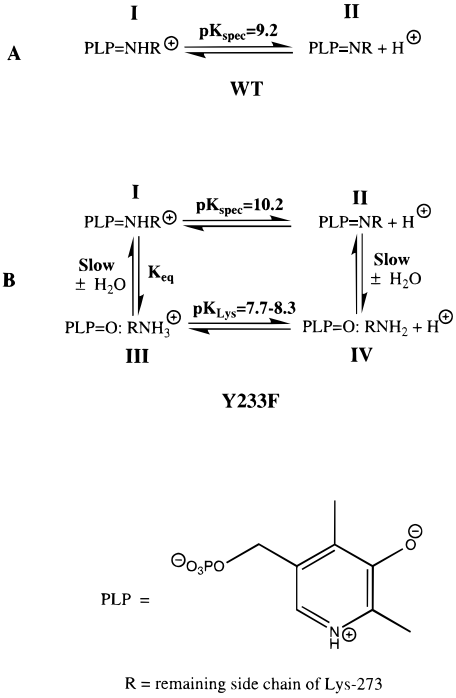

[a] While the WT equilibrium is dominated by a single pK_a between the protonated Schiff base (I) and the unprotonated Schiff base (II) in panel A, Y233F exists as four species governed by two pK_as (I to II and III to IV) and two equilibria for the slow hydrolysis reactions of I to III and II to IV.

and the cofactor in ACC synthase cannot pull PLP into the conformation that exists in AATase (Scheme 4). The consequences are that k_{cat} is relatively unchanged in the mutant ACC synthase, since the position of the proton abstracting ϵ-NH_2 of Lys273 with respect to the C_α-H of SAM is relatively unchanged. The K_M value is 24-fold higher in the mutant enzyme possibly due to a minor misorientation of PLP in the absence of the hydrogen bond.

The pH dependence of the spectral change resulting from the tyrosine to phenylalanine mutation is also different for the two enzymes. Both the spectrophotometrically and kinetically determined pK_as rise from 6.8 in WT AATase to 8.6 with the Y225F mutation. The absorbance peaks of the protonated Schiff base form of both WT and Y225F AATase are found at 430 nm; however, the deprotonated Schiff base absorbs at 360 nm in the WT, but at 390 nm in the Y225F mutant. While the latter peak is tantalizingly close to the absorbance maximum of free PLP, the species was proven convincingly to be a Schiff base condensate with Lys258 by isotope edited classical Raman spectroscopy (*41*). The Y233F mutation in ACC synthase, by contrast with AATase, results in a separation of the kinetic and the spectral pK_a (8.7 *vs* 10.2, respectively) (Figures 5 and 8, Table 1). This, to the best of our knowledge, is unprecedented for vitamin B_6-dependent enzymes. Moreover, the extinction coefficient for the protonated form of Y233F ACC synthase is only about one-half of that of wild-type. The absorbance peaks of WT and Y233F ACC synthases are both at 420 nm (low pH) and 390 nm (high pH). The latter peak is consistent with PLP bound either as the free aldehyde or as the imine (*41*).

It has not yet been feasible to prepare sufficient quantities of ACC synthase for Raman spectroscopy, so this issue

Table 2: Spectrophotometric Characteristics of Wild-Type and Active Site Tyrosine Mutant Forms of AATase and ACC Synthase

		low pH		high pH	
	pK_{spec}	λ_{max} (nm)	fraction existing as Form I (Scheme 7)	λ_{max} (nm)	fraction existing as Form II (Scheme 7)
AATase (WT)[a]	7.0	430	1	358	1
AATase (Y225F)[a]	8.6	435	1	386	1
ACC synthase (WT)	9.2	420	1	390	1
ACC synthase (Y233F)[b]	10.2	420	0.6[c]	390	0.6[d]

[a] Goldberg et al. (*25*). [b] The spectral and kinetic pK_as differ significantly for this mutant. See text. [c] [I]/([I] + [III]) calculated from the relative absorbance at 420 nm. [d] This is the same fraction as estimated from the low pH spectrum (footnote c) with the assumption that the aldehyde and imine forms interconvert slowly. See text.

Table 3: Simulations of the pH Dependence of k_{cat}/K_M for Y233F ACC Synthase[a]

assumed values		calculated values		
K_{eq}	pK_{SAM}	$(k_{cat}/K_M)^{III}$ ($\times 10^{-5}$ M^{-1} s^{-1})	$(k_{cat}/K_M)^{I}$ ($\times 10^{-3}$ M^{-1} s^{-1})	pK_{Lys} (Lys-NH_3^+)
0.6	8.3	9.3 (±1.1)	4.7 (±4.0)	7.7 (±0.1)
	7.7	2.1 (±0.1)	0.3 (±5.2)	8.4 (±0.1)
0.8	8.3	7.9 (±1.0)	5.3 (±4.5)	7.7 (±0.1)
	7.7	1.8 (±0.1)	0.4 (±5.9)	8.4 (±0.1)
1.0	8.3	7.0 (±0.9)	6.0 (±5.0)	7.7 (±0.1)
	7.7	1.6 (±0.1)	0.4 (±6.5)	8.4 (±0.1)
1.2	8.3	6.4 (±0.8)	6.5 (±5.5)	7.7 (±0.1)
1.4	8.3	6.0 (±0.7)	7.1 (±6.0)	7.7 (±0.1)
	7.7	1.4 (±0.1)	0.5 (±7.8)	8.4 (±0.1)

[a] The data (see Figure 8) were fitted to the three pK_a bell-shape curve described by eq 7. pK_{spec} was set to the spectrally determined value of 10.2.

cannot yet be resolved definitely. We assume for the purpose of the following discussion that the inactive high pH form of the Y233F mutant is the aldehyde (Scheme 7B, structure IV), but cannot rule out that it is the Schiff base in slow prototropic equilibrium with the bound substrate. The spectra of WT and Y225F mutant AATase are compared in Table 2. The low value of the 420 nm extinction coefficient for the low pH form of Y233F ACC synthase suggests that about one-half of the total enzyme exists in the free aldehyde form [Scheme 7B, ([III] + [IV])/([II] + [I])] contrasting with AATase in this respect (Table 2). These observations lead to the following explanation to account for the lack of coincidence of spectrophotometric with kinetic pK_a values in this mutant enzyme. It is proposed that the aldehyde forms of PLP in the mutant (III and IV) interconvert *slowly* with the Schiff base forms (I and II) and that the major reacting species are the neutral amino form of SAM and III. The pH dependence of k_{cat}/K_M is described by eq 7:

$$(k_{cat}/K_M)^{obs} = \frac{1}{1+10^{(pK_{SAM}-pH)}}\frac{1}{1+K_{eq}} \times \left\{\frac{(k_{cat}/K_M)^{III}}{1+10^{(pH-pK_{Lys})}}K_{eq} + \frac{(k_{cat}/K_M)^{I}}{1+10^{(pH-pK_{spec})}}\right\} \quad (7)$$

Structures I and III and pK_{Lys} are defined in Scheme 7. K_{eq} = [III]/[I] and pK_{spec} = the spectrophotometric pK_a of 10.2. The vertical equilibria in Scheme 7B are established with a pseudo-first-order rate constant that is much less than either value of k_{cat}/K_M [SAM-NH_2]; therefore, the rate of disap-

pearance of SAM is effectively described by two parallel reactions, i.e., the two terms within the bracket.

Simulations. The spectrophotometric data at pH 8.26 (Figure 5) show that $K_{eq} \approx 1$ (Scheme 7B). The K_{eq} value was varied from 0.6 to 1.4. The pK_a of SAM (pK_{SAM}) determined directly is 8.0 ± 0.2, and this value was allowed to vary from 7.7 to 8.3. The values of $(k_{cat}/K_M)^I$, $(k_{cat}/K_M)^{III}$, and pK_{Lys} (that of the ϵ-NH_3^+ of Lys273 in the III to IV prototropy) were treated as adjustable parameters. The best results as judged from the lowest values of the reduced sum of squares are found in Table 3. The main findings are that the pK_a of the lysine residue is reciprocally related to that assigned to SAM, i.e., pK_{SAM} = 8.3, pK_{Lys} = 7.7 and pK_{SAM} = 7.7, pK_{Lys} = 8.4, and that greater than 99% of the reaction flux is through species III rather than I, contrasting sharply with other PLP-dependent enzymes in this respect. The curve in Figure 8 is calculated from eq 7 with the following parameter values: K_{eq} = 1.0, pK_{SAM} = 8.3, pK_{spec} = 10.2, pK_{Lys} = 7.7, $(k_{cat}/K_M)^I = 6.0 \times 10^3\ M^{-1}\ s^{-1}$, and $(k_{cat}/K_M)^{III} = 7.0 \times 10^5\ M^{-1}\ s^{-1}$. The fit is excellent and explains well the unique discordance between the spectral and kinetic pK_a values.

ACKNOWLEDGMENT

The authors thanks Dr. Jonathan M. Goldberg for stimulating discussion and for constructing a homology model of ACC synthase and Brenda Ng for providing purified Y85A ACC synthase.

REFERENCES

1. Yang, S. F., and Hoffman, N. E. (1984) *Annu. Rev. Plant Physiol. 35*, 155−189.
2. Alexander, F. W., Sandmeier, E., Mehta, P. K., and Christen, P. (1994) *Eur. J. Biochem. 219*, 953−960.
3. Adams, D. O., and Yang, S. F. (1979) *Proc. Natl. Acad. Sci. U.S.A. 76*, 170−174.
4. Ramalingam, K., Lee, K.-M., Woodard, R. W., Bleecker, A. B., and Kende, H. (1985) *Proc. Natl. Acad. Sci. U.S.A. 82*, 7820−7824.
5. Van der Straeten, D., Van, W. L., Goodman, H. M., and Van, M. M. (1990) *Proc. Natl. Acad. Sci. U.S.A. 87*, 4859−4863.
6. Nakajima, N., Mori, H., Yamazaki, K., and Imaseki, H. (1990) *Plant Cell Physiol. 31*, 1153−1163.
7. Dong, J.-G., Kim, W. T., Yip, W.-K., Thompson, G. A., Li, L., Bennett, A. B., and Yang, S. F. (1991) *Planta 185*, 38−45.
8. Sato, T., Oeller, P. W., and Theologis, A. (1991) *J. Biol. Chem. 266*, 3752−3759.
9. White, M. F., Vasquez, J., Yang, S. F., and Kirsch, J. F. (1994) *Proc. Natl. Acad. Sci. U.S.A. 91*, 12428−12432.
10. Hohenester, E., White, M. F., Kirsch, J. F., and Jansonius, J. N. (1994) *J. Mol. Biol. 243*, 947−949.
11. Yip, W.-K., Dong, J.-G., and Yang, S. F. (1991) *Plant Physiol. 95*, 251−257.
12. Nakajima, N., and Imaseki, H. (1986) *Plant Cell Physiol. 27*, 969−980.
13. Li, N., and Mattoo, A. K. (1994) *J. Biol. Chem. 269*, 6908−6917.
14. Satoh, S., Mori, H., and Imaseki, H. (1993) *Plant Cell Physiol. 34*, 753−760.
15. Gloss, L. M., and Kirsch, J. F. (1995) *Biochemistry 34*, 3999−4007.
16. Goldberg, J. M., and Kirsch, J. F. (1996) *Biochemistry 35*, 5280−5291.
17. Brouwer, A. C., and Kirsch, J. F. (1982) *Biochemistry 21*, 1302−1307.
18. Bazelyansky, M., Robey, E., and Kirsch, J. F. (1986) *Biochemistry 25*, 125−130.
19. Blacklow, S. C., Raines, R. T., Lim, W. A., Zamore, P. D., and Knowles, J. R. (1988) *Biochemistry 27*, 1158−1167.
20. Privalle, L. S., and Graham, J. S. (1987) *Arch. Biochem. Biophys. 253*, 333−340.
21. Yip, W.-K., Dong, J.-G., Kenny, J. W., Thompson, G. A., and Yang, S. F. (1990) *Proc. Natl. Acad. Sci. U.S.A. 87*, 7930−7934.
22. Ellis, K. J., and Morrison, J. F. (1982) *Methods Enzymol. 87*, 405−426.
23. Jenkins, W. T., and Sizer, I. W. (1957) *J. Am. Chem. Soc. 79*, 2655−2656.
24. Jenkins, W. T., Yphantis, D. A., and Sizer, I. W. (1959) *J. Biol. Chem. 234*, 51−57.
25. Goldberg, J. M., Swanson, R. V., Goodman, H. S., and Kirsch, J. F. (1991) *Biochemistry 30*, 305−312.
26. Wente, S. R., and Schachman, H. K. (1987) *Proc. Natl. Acad. Sci. U.S.A. 84*, 31−35.
27. Herold, M., and Kirschner, K. (1990) *Biochemistry 29*, 1907−1913.
28. Onuffer J. J., and Kirsch, J. F. (1994) *Protein Eng. 1*, 413−424.
29. Kallen, R. G., Korpela, T., Martell, A. E., Matsushima, Y., Metzler, C. M., and Metzler, D. E. (1985) in *Transaminases* (Christen, P., and Metzler, D. E. Eds.) pp 37−108, Wiley, New York.
30. Gloss, L. M., and Kirsch, J. F. (1995) *Biochemistry 34*, 3990−3998.
31. Tai, C.-H., Nalabolu, S. R., Simmons, J. W., III, Jacobson T. M., and Cook, P. F. (1995) *Biochemistry 34*, 12311−12322.
32. Connor, W. A., Jones, M. M., and Tuleen, D. L. (1965) *Inorg. Chem. 4*, 1129−1133.
33. Rottmann, W. H., Peter, G. F., Oeller, P. W., Keller, J. A., Shen, N. F., Nagy, B. P., Taylor, L. P., Campbell, A. D., and Theologis, A. (1991) *J. Mol. Biol. 222*, 937−961.
34. McPhalen, C. A., Vincent, M. G., Jansonius, J. N. (1992) *J. Mol. Biol. 225*, 495−517.
35. Malashkevich, V. N., Strokopytov, B. V., Borisov, V. V., Dauter, Z., Wilson, K. S., and Torchinsky, Y. M. (1995) *J. Mol. Biol. 247*, 111−124.
36. Okamoto, A., Higuchi, T., Hirotsu, K., Kuramitsu, S., and Kagamiyama, H. (1994) *J. Biochem. (Japan) 116*, 95−107.
37. Jager, J., Moser, M., Sauder, U., and Jansonius, J. N. (1994) *J. Mol. Biol. 239*, 285−305.
38. Hardy, L. W., and Kirsch, J. F. (1984) *Biochemistry 23*, 1275−1282.
39. Simopoulos, T. T., and Jencks, W. P. (1994) *Biochemistry 33*, 10375−10380.
40. Kirsch, J. F., Eichele, G., Ford, G. C., Vincent, M. G., Jansonius, J. N., Gehring, H., and Christen, P. (1984) *J. Mol. Biol. 174*, 497−525.
41. Goldberg, J. M., Zheng, J., Deng, H., Chen, Y. Q., Callender, R., and Kirsch, J. F. (1993) *Biochemistry 32*, 8092−8097.

BI971625L